Journal of the Mechanical Behavior of Biomedical Materials **67,** 110-116 (2017)

Evaluation of the mechanical properties of powder metallurgy Ti-6Al-7Nb alloy

L. Bolzoni[1*], E.M. Ruiz-Navas[2], E. Gordo[2]

[1]WaiCAM (Waikato Centre for Advanced Materials), The University of Waikato

Private Bag 3105, 3240 Hamilton – New Zealand

[2]Department of Materials Science and Engineering, University Carlos III of Madrid,

Avda. de la Universidad, 30, 28911 Leganes, Madrid - Spain

*bolzoni.leandro@gmail.com

Abstract

Titanium and its alloys are common biomedical materials owing to their combination of mechanical properties, corrosion resistance and biocompatibility. Powder metallurgy (PM) techniques can be used to fabricate biomaterials with tailored properties because changing the processing parameters, such as the sintering temperature, products with different level of porosity and mechanical performances can be obtained. This study addresses the production of the biomedical Ti-6Al-7Nb alloy by means of the master alloy addition variant of the PM blending elemental approach. The sintering parameters investigated guarantee that the complete diffusion of the alloying elements and the homogenization of the microstructure is achieved. The sintering of the Ti-6Al-7Nb alloy induces a total shrinkage between 7.4% and 10.7% and the level of porosity decreases from 6.2% to 4.7% with the increment of the sintering temperature. Vickers hardness (280-300 HV30) and tensile properties (different combination of strength and elongation around 900 MPa and 3%) are achieved.

Keywords: titanium alloy, Ti-6Al-7Nb, powder metallurgy, homogeneous microstructure, tensile properties

1. Introduction

Biomaterials are commonly classified as a function of their intrinsic nature as polymeric, ceramics/glasses and metallic biomaterials and, thus, employed to fabricate specific surgical, orthopaedics and dentistry products and prostheses. Specifically, polymeric-based materials are characterised by a high degree of flexibility which permits to tailor their property for particular applications. High compressive strength and wear resistance combined with inert behaviour and pleasing aesthetic appearance are the properties for which biomedical ceramics and glasses are renowned. Relative ease of fabrication as well as high strength and resistance to fracture are the main reasons for which metals continue to be used in biomedical applications (Narayan, 2009). Titanium is generally preferred to other metallic biomaterials due to the combination of properties (i.e. low density, relatively low Young modulus, superior biocompatibility and corrosion resistance) that can provide (Niinomi, 1998). When it comes to the introduction of new orthopaedic materials, until recently the adaptation of existing materials was the mainstream approach taken (Long and Rack, 1998). Therefore, concerning titanium-based materials, elemental titanium and the most well-known Ti-6Al-4V alloy were the first to be introduced and used for biomedical applications. Nevertheless, because of the concerns about the effect of the dissolution of the chemical elements, especially the formation of vanadium ions, and the possible toxic effect (Khan et al., 1999) alternatives were proposed. In particular, the Ti-6Al-7Nb alloy was developed with the aim of replacing the Ti-6Al-4V alloy due to its potential cytotoxicity and adverse reaction with the body tissues. Ti-6Al-7Nb alloy has equivalent mechanical performances to the Ti-6Al-4V alloy but improved biocompatibility (Semlitsch et al., 1995). The Ti-6Al-7Nb alloy was developed primarily for the production of cementless anchored hip prosthesis stems and elastic deformable cup shells (Semlitsch et al., 1985) and it was primarily produced by ingot metallurgy plus forging (Semlitsch et al., 1992). In recent years, a new class of titanium alloys, known as beta titanium alloys, targeting the reduction of the intrinsic stiffness of the material has also been

developed by primarily adding biocompatible beta stabilisers such as zirconium and tantalum. A comprehensive description can be found in the literature (Narayan, 2009; Niinomi, 2002). The processing of titanium and its alloys by means of powder metallurgy (PM) techniques is claimed to be a suitable way to reduce the fabrication cost of titanium products where the master alloy (MA) addition variant of the blending elemental approach has been identified has the cheapest way to obtain titanium alloys with the desired composition (Hurless and Froes, 2002). The production of the Ti-6Al-7Nb alloy by PM techniques has been done considering different methods like hot-press and injection moulding (Itoh et al., 2007). The aim of this work is to study the suitability of the production of the Ti-6Al-7Nb alloy by combining the MA approach and the cheapest PM route (i.e. press and sinter) and evaluate its tensile behaviour. In particular, the microstructural features, physical, chemical and mechanical properties achievable by changing the sintering temperature are studied and correlated with the processing parameters and among themselves.

2. Materials and methods

2.1 Production and characterisation of the Ti-6Al-7Nb powder

The starting materials bought for the development of the study are a hydride-dehydride (HDH) elemental titanium powder and a niobium:aluminium:titanium (Nb:Al:Ti) master alloy, both supplied by GfE Gesellschaft für Elektrometallurgie mbH. The Nb:Al:Ti master alloy was in the form of granules (maximum particle size < 800 μm) and had a ratio between the elements of 60:35:5 (percentages in weight). Because, as delivered, the master alloy was not suitable for its mixing with elemental titanium, the particle size was reduced by high energy ball milling and the ratio of the alloying elements adjusted to the desired composition by adding an elemental aluminium spherical powder bought from Sulzer Metco Ltd. The detailed route employed to obtain the Ti-6Al-7Nb powder is available in the literature (Bolzoni et al., 2012).

Basic characteristics of the produced Ti-6Al-7Nb powder were analysed and they included particle size, contents of interstitial elements and morphology/composition. Specifically, the particle size distribution and, hence, the maximum particle size (D_{max}) was determined by means of a laser beam Mastersizer 2000 particle size analyser. Concerning the interstitials, oxygen and nitrogen contents were measured following the specifications of the ASTM: E1409 standard using a LECO TC500 equipment. The morphology/composition of the powder was checked using a Philips XL–30 SEM in backscattered mode.

2.2 Consolidation and characterisation of the sintered Ti-6Al-7Nb components

The consolidation of the powder was done by means of a uniaxial press combined with a floating die whose walls were lubricated using zinc stearate. It is worth mentioning that, intentionally, no lubricant was added directly to the powder in order to prevent or, at least, limit as much as possible the contamination of the powder. Dogbones samples with standardised dimensions (ASTM: B925) for tensile tests were cold uniaxial pressed setting the compaction pressure to 700 MPa. The green components were sintered in a high vacuum tubular furnace (approximately 10^{-5} mbar) while laid on zirconia balls once again to prevent/limit interaction with the sintering substrate. The processing parameters to sinter the components were: sintering temperature range between 1250ºC and 1350ºC, dwell time at maximum temperature of 120 min and heating/cooling rates of 5ºC/min.

The metallographic route used to prepare the samples for the microstructural analysis included grinding with SiC papers of different granulometry, polishing with an alumina-based solution (1 μm) and fine polishing with silica gel. The microconstituents were revealed by means of chemical etching using Kroll reactant (3 ml HF + 6 ml HNO_3 + 100 ml H_2O). Microstructural analysis was carried out on an Olympus GX71 light optical microscope whilst the homogeneous distribution of the alloying elements and the fractographic study were done on the Philips XL-30 SEM.

The variation of the dimensions experienced by the samples during the sintering step was considered and estimated because they are important industrial factors to take into account when designing a new component to be produced by means of PM techniques. The values of the density of the sintered samples was measured by means of the water displacement method. The total residual porosity (P_{res}) was calculated as a difference between the density measured and the nominal value of the density of the Ti-6Al-7Nb alloy, that is 4.52 g/cm^3 (Boyer et al., 1998).

It is well known that the amount of interstitials dissolved greatly influence the mechanical properties of titanium (Finlay and Snyder, 1950; Jaffee and Campbell, 1949; Jaffee et al., 1950), therefore, oxygen and nitrogen contents of the sintered samples were measured using the same equipments and conditions previously specified for the starting powder.

Regarding to the mechanical characterisation, Vickers hardness measurements were done on the cross section of the samples by means of a Wilson Wolpert Universal Hardness DIGI-TESTOR 930 tester performing HV30 measurements. Ultimate tensile strength (UTS) and elongation at fracture values were obtained using a MicroTest universal machine equipped with a load cell of 50 KN and a Hottinger Baldwin Messtechnik, type DD1 extensometer. Tensile tests were performed following the ASTM: E8 standard applying a crosshead speed of 1 mm/min. In order to limit the experimental error, the (dynamics) elastic modulus was determined using the equation $v = \sqrt{E/\rho}$ which correlates the Young modulus (E) with the speed of sound in the material (v) and the density (ρ). In particular, the speed of sound was measured by means of an ultrasonic transducer (Grindosonic) having a frequency range in between 20 Hz and 100 KHz and an accuracy better than 0.005%.

3. Results and discussion

3.1 Characterisation of the Ti-6Al-7Nb powder

Some basic characteristics (i.e. particle size distribution and contents of interstitials) of the powders used in this study are shown in Table 1 whilst the morphology/composition can be seen in the micrographs shown in Figure 1.

Table 1. Basic characteristics of the Ti-6Al-7Nb powder employed in this study.

Feature	Ti:6Al:7Nb
Mean particle size, D_{50} [µm]	40.4 ± 3.52
Maximum particle size, D_{MAX} [µm]	81.9 ± 5.74
O [wt.%]	0.39 ± 0.01
N [wt.%]	0.017 ± 0.001

From the particle size distribution data shown in Table 1, it can be noticed that the produced Ti-6Al-7Nb powder is characterised by a D_{90} parameter of 81.94 µm and, thus, the powder can be classified as a 170 mesh powder (D < 90 µm). Oxygen and nitrogen contents are slightly lower than 0.40 wt.% and 0.02 wt.%, respectively. In comparison to the typical interstitials contents of the wrought Ti-6Al-7Nb alloy (ASTM: F1295 or IMI 367) (Boyer et al., 1998; Henry, 2009), on the one side the produced Ti-6Al-7Nb powder has higher oxygen content and this will affect the mechanical behaviour of the sintered components. On the other side, the amount of nitrogen is lower than the limit specified for the wrought material.

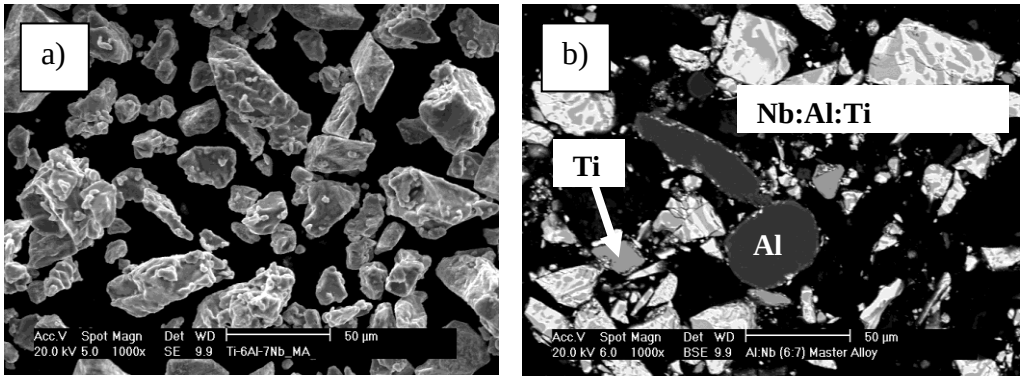

Figure 1. Micrographs showing the features of the Ti-6Al-7Nb powder: a) morphology and b) composition of the Ti-6Al-7Nb powder.

The micrograph shown in Figure 1 a) confirms that the Ti-6Al-7Nb powder is actually characterised by an irregular morphology due to the fact that it was produced by means of the HDH comminution process. The irregular morphology is paramount because the powder is consolidated by means of cold uniaxial pressing and, thus, undergoes particles rearrangement as well as elastic and plastic deformation. This results into mechanical interlocking between the powder particles (i. e. green strength) (German, 1994; Schatt and Wieters, 1997) and guarantees the handling of the shaped components. From Figure 1 b) it can be seen that the three powders used to produce the Ti-6Al-7Nb alloy could be clearly identified using the BSE mode due to the different atomic number of the elements. From the micrograph shown in Figure 1 b), it can also be seen that the shape of the elemental aluminium powder added to adjust the composition is not perfectly spherical but slightly deformed due to the fact that the powder was milled altogether with the Nb:Al:Ti master alloy. Moreover, the particle size of the Nb:Al:Ti master alloy is approximately 50 μm, which means that was effectively reduced by the high energy ball milling step, and its morphology is mainly angular.

3.2 Characterisation of the sintered Ti-6Al-7Nb components

The evolution of the microstructure and porosity with the sintering temperature was studied by analysing the microstructural features at the optical microscope. Representative examples of the microstructure of the sintered Ti-6Al-7Nb alloy are shown in Figure 2 where it can be seen that the microconstituents that compose the microstructure of the sintered Ti-6Al-7Nb component are elongated α grains and α + β lamellae distributed throughout the microstructure. This is the typical lamellar microstructure of α + β titanium alloys slow cooled from a temperature above their β transus.

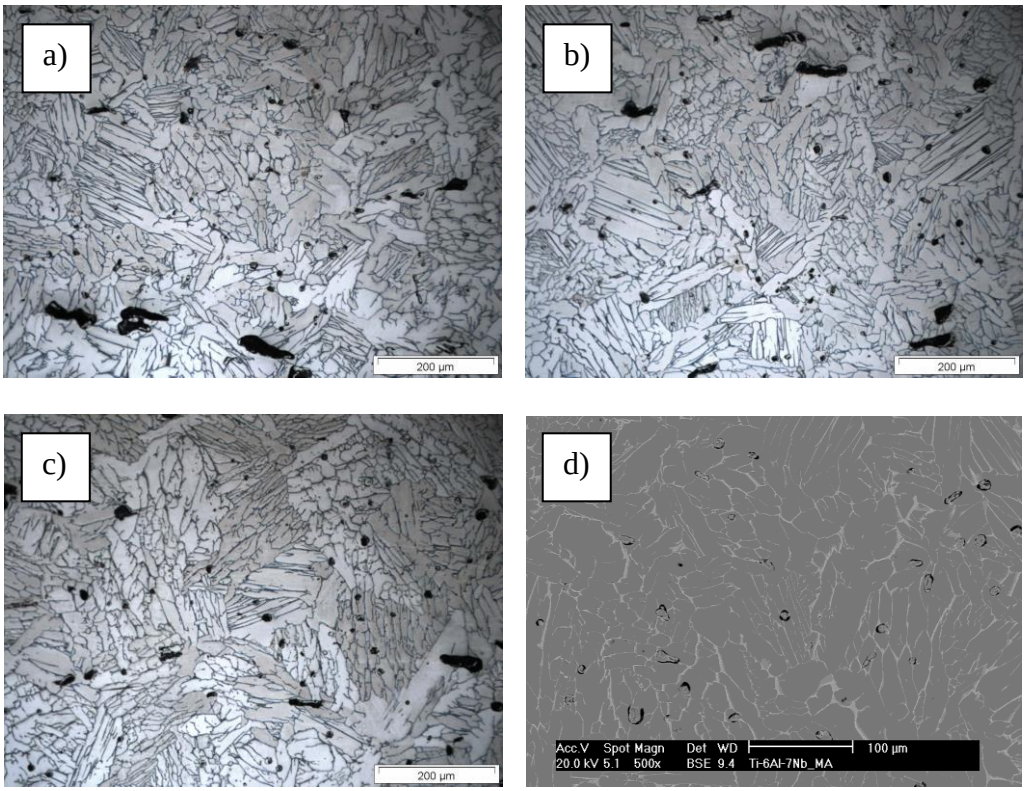

Figure 2. Optical micrographs of the microstructure of the sintered Ti-6Al-7Nb alloy: a) 1250ºC, b) 1300ºC and c) 1350ºC, and d) BSE-mode SEM micrograph of the alloy sintered at 1300ºC.

Generally, there is a coarsening of the microconstituents with the increment of the sintering temperature due to the higher thermal energy available in the system for grain growth, resulting in an increase in grain size of the sintered Ti-6Al-7Nb alloy. Specifically, the size of the α grains becomes larger as the higher sintering temperature leads to the formation of coarser prior β grains during sintering, β grains from which α grains nucleate (134±17, 147±14 and 165±20 for the materials sintered at 1250ºC, 1300ºC and 1350ºC, respectively). Simultaneously, there is an increment in size of the α + β lamellae (11±3, 17±10 and 20±8 for the materials sintered at 1250ºC, 1300ºC and 1350ºC, respectively). From Figure 2, the other feature characterising the microstructure of the sintered Ti-6Al-7Nb alloy is the residual porosity and it can be seen that it is closed and isolated porosity. The total volume percentage of residual porosity decreases with the increment of the sintering temperature. Besides, the

pores are mainly spherical, even though some relatively large elongated pores are still present. Furthermore, the average pore size increases with the processing temperature. The presence of irregular pores and the increment of the pore size is because during the second stage of sintering, after that the interparticle boundaries had disappeared, the pores tend to coalesce reducing their percentage but increasing the size of the remaining pores. Summarising, the prior β grain size increases and the volumetric percentage decreases with the increment of the sintering temperature.

Although the residual porosity could affect negatively the mechanical response of the sintered Ti-6Al-7Nb alloy, these pores are actually beneficial for osteoconduction and the ability to form apatite (Fujibayashi et al., 2004) where the optimal pore diameter distribution lies between 150 μm and 500 μm (Hulbert et al., 1972). The microstructure of the sintered samples was also analysed at the SEM in order to check the homogeneity of the materials, which is paramount because the alloying elements are added by means of a master alloy and the sintering temperature has to be high enough to guarantee their diffusion. A possible presence of undissolved aluminium and niobium will affect considerably the biological response (Khan et al., 1996) such as inhibition of apatite formation and/or formation of debris leading to loosening of the implants due to osteolysis. Because no significant difference were found during this analysis, the micrograph of the samples sintered at 1300ºC is shown as representative example in Figure 2 d). The backscattered mode of the SEM permits to differentiate the elements present in a materials as a function of their atomic number which, therefore, will appear in a micrograph with different brightness. From the micrographs shown in Figure 2 d) it can be noticed that the microstructure of the Ti-6Al-7Nb components is composed of a grey phase, which is α, and a bright phase (i.e. β phase) due to the presence of the niobium as β stabiliser. Furthermore, the distribution of these two phases is homogeneous throughout the whole microstructure and not undissolved master alloy particles could be found. This indicates that, actually, with the sintering temperatures employed the complete

diffusion and homogeneous distribution of the alloying elements is reached. From the EDS analysis carried out on the samples, it was found that the mean atomic percentage of aluminium is 10.2 at.% whilst that of niobium is 3.6 at.%, and titanium is the base. Moreover, it can be stated that the pressed and sintered components respect the limits of the alloying elements specified for the ASTM: F1295 alloy (Boyer et al., 1998) and are, therefore, comparable to the wrought material in terms of chemical composition. On average, the chemical composition of the α-Ti and β-Ti phases of the sintered Ti-6Al-7Nb components is 87.7Ti-10.4Al-1.9Nb and 81.3Ti-5.4Al-13.3Nb in atomic percentage, respectively. The α-Ti and β-Ti phases are, respectively, Al and Nb-rich as aluminium and niobium are alpha and beta stabilisers. These results are in agreement with the Ti-Nb binary phase diagram which indicates that the maximum solubility of niobium in α-Ti is 2.2 ± 0.5 at.% (Murray, 1987). After the shaping of the powder, the components are characterised by a green density of approximately 86.0 ± 1.2%. The variation of the physical properties (i.e. shrinkage, density and residual porosity) of the sintered Ti-6Al-7Nb alloy with the sintering temperature are shown in Figure 3.

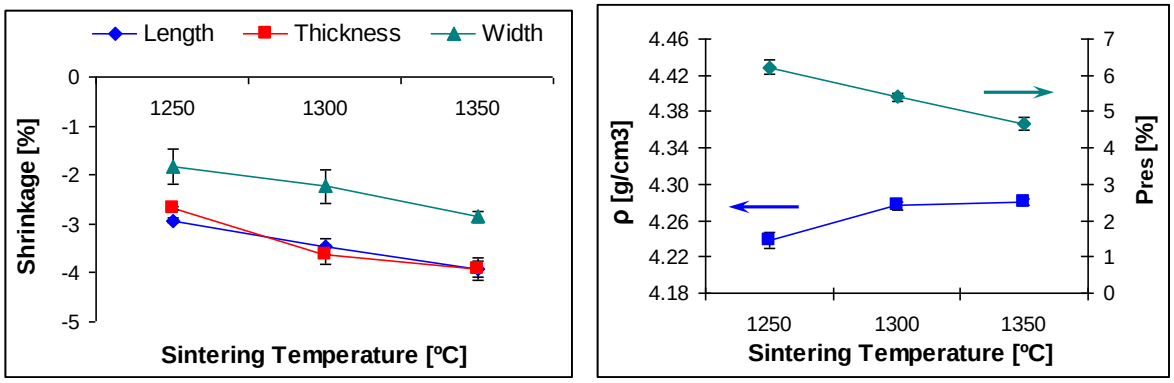

Figure 3. Variation of the physical properties of the sintered Ti-6Al-7Nb alloy with the sintering temperature: a) shrinkage and b) density and residual porosity.

The sintering of the green components induces a reduction of their dimension and, therefore, the samples undergo shrinkage (Figure 3 a). In particular, the contraction of the dimensions

(length, width and thickness) increases with the increment of the processing temperature ranging from 2% to 4% as a function of the sintering temperature selected. Moreover, it can be noticed that the shrinkage of the dimensions of the components is quite homogeneous with the exception of the variation of the width which is somewhat lower. The absolute values of these variations are useful when design a new components. In particular, from the results shown in can be estimated that the dimensions of the prosthesis produced by PM should be 10% bigger than the required because the component will shrink during its sintering. From Figure 3 b) it can be seen that the density of the Ti-6Al7Nb alloy increases with the increment of the processing temperature and, conversely, the total volumetric percentage of residual porosity decreases. The value of the corresponding relative density (i.e. 94-96%) are common values for titanium alloys obtained by pressing and sintering (Abkowitz and Rowell, 1986; Bolzoni et al., 2013; Ivasishin, 2005).

Table 2 shows the results of the chemical analysis carried out on sintered Ti-6Al-7Nb components where it can be noticed that there is some oxygen and nitrogen pick-up with respect to the initial powder (Table 1) and the nitrogen pick-up is somewhat more pronounced. Nonetheless, the oxygen content is approximately 0.40 wt.% whereas that of nitrogen is as maximum 0.035 wt.%. The interstitials pick-up can be attributed to the handling of the powder and the air trapped into the green samples and, therefore, the contaminants adsorbed on the surface or trapped in the green body diffuse inside the material during the sintering step. It is expected that the total amount of oxygen dissolved inside the titanium lattice (0.4%) shifts the actual β transus of the Ti-6Al-7Nb alloy by about 20ºC and therefore influences the initial nucleation of the α grains from the prior β grains with respect to the wrought Ti-6Al-7Nb alloy. In the study, as the sintered materials have comparable oxygen content (Table 2), the coarsening of the microconstituents is dictated by the sintering temperature rather than by the oxygen content.

Table 2. Chemical analysis results (i.e. oxygen and nitrogen contents) of sintered Ti-6Al-7Nb components.

Processing conditions	**Chemical analysis**	
	Oxygen [wt.%]	*Nitrogen [wt.%]*
1250ºC-2h	0.38 ± 0.02	0.032 ± 0.001
1300ºC-2h	0.41 ± 0.01	0.033 ± 0.001
1350ºC-2h	0.39 ± 0.01	0.035 ± 0.001

The results of the Vickers hardness measurements of the sintered Ti-6Al-7Nb alloys are shown in Figure 4 where, as for the relative density, the hardness of the Ti-6Al-7Nb components increases with the processing temperature. This is mainly due to the reduction of the residual porosity present in the microstructure. However, it is well known that the higher the amount of interstitials dissolved into titanium the higher its hardness (Finlay and Snyder, 1950; Jaffee and Campbell, 1949; Jaffee et al., 1950). Thus, there is also a contribution from the slight differences in chemical composition because the samples sintered at 1300ºC have somewhat higher oxygen than those processed at 1250ºC. The values of hardness obtained for the sintered Ti-6Al-7Nb components are lower than that found by Semlitsch et al. (350 HV) in the wrought alloy (Semlitsch et al., 1995) but comparable to the value specified for IMI 367 medical devices (290 HV) (Henry, 2009).

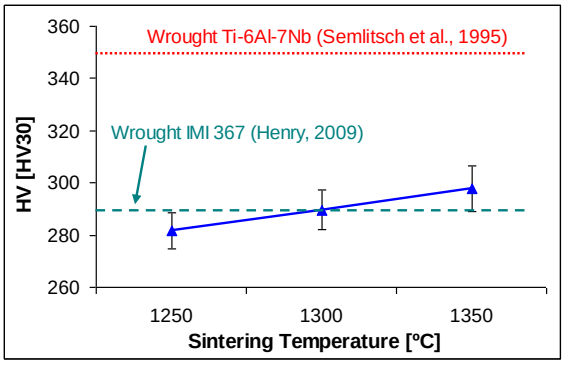

Figure 4. Variation of the Vickers hardness of the sintered Ti-6Al-7Nb alloy with the sintering temperature compared to the wrought Ti-6Al-7Nb alloy.

From the tensile stress-strain curves presented in Figure 5 a), it can be seen that the Ti-6Al-7Nb sintered components show similar mechanical behaviour independently of the sintering temperature employed and, thus, they are characterised by similar elastic modulus. Furthermore, the sintered components undergo an elastic deformation up to approximately 700 MPa and then start to deform plastically.

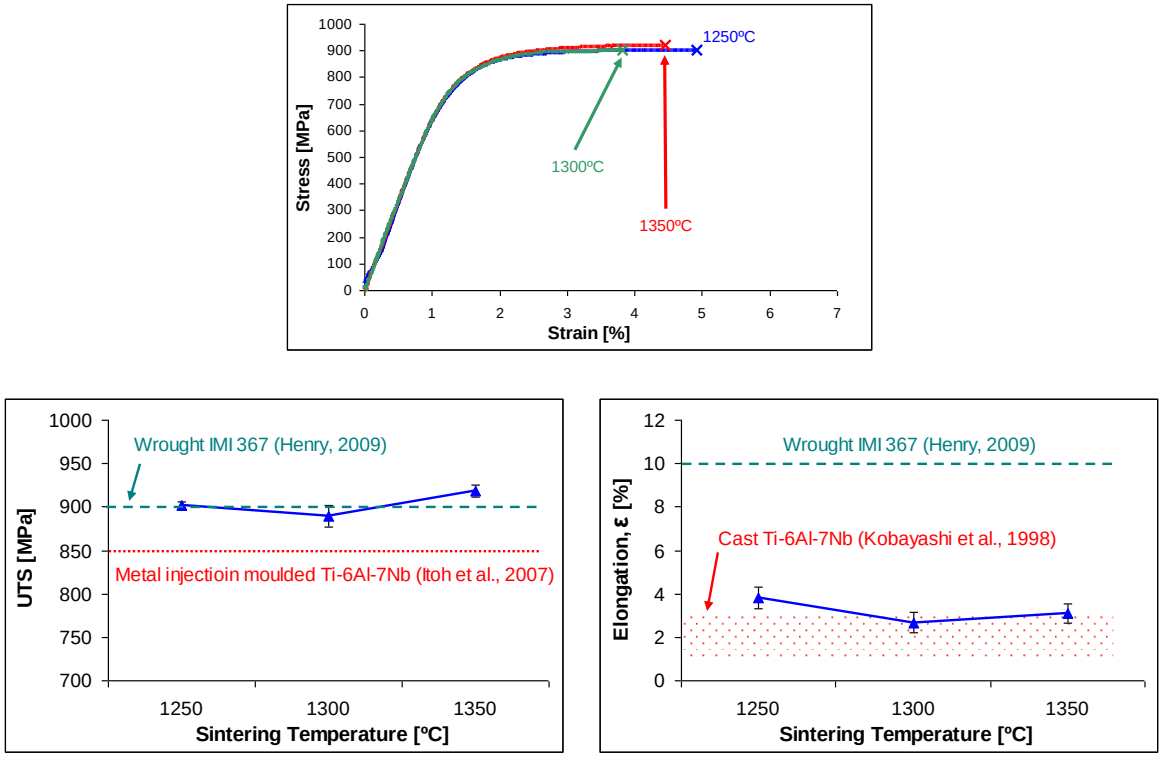

Figure 5. Mechanical behaviour of the sintered Ti-6Al-7Nb alloy compared to the wrought Ti-6Al-7Nb alloy: a) stress-strain curves, b) ultimate tensile strength and c) elongation at fracture.

The ultimate tensile strength on the sintered components (Figure 5 b) does not seem to be greatly influenced by the sintering temperature because the strength is about 900±14 MPa (measured in, at least, three samples for each condition) for all the sintering temperatures studied. This seems to indicate that the positive effect of the reduction of the residual porosity and of the strengthening effect of the interstitials is balanced by the grain growth and the coarsening of the residual porosity induced by the higher processing temperature. As

indicated in Figure 5 b), the strength of the sintered Ti-6Al-7Nb components is similar to that of the wrought (ASTM: F1295 or IMI 367) alloy, that is 900 MPa, and higher than that obtained by Itoh et al. (Itoh et al., 2007) (approximately 850 MPa) when processing a spherical elemental titanium powder mixed with an Al:Nb master alloy by metal injection moulding and using a similar sintering temperature range. The sintered Ti-6Al-7Nb components have comparable strength to the wrought alloy even though of the presence of the residual porosity. This is because of the high amount of oxygen of the sintered alloy with respect to the wrought material. The elongation at fracture (Figure 5 c) of the alloy slightly decreases with the sintering temperature although the samples processed at 1300ºC (i.e. 2.7±0.5%) have somewhat lower strain than those sintered at 1350ºC (i.e. 3.1±0.9%) and 1250ºC (i.e. 3.8±1.0%). This behaviour is due to the higher oxygen content found in the components sintered at 1300ºC (Table 2) in comparison to the other sintering conditions because oxygen decreases the ductility of titanium (Finlay and Snyder, 1950; Jaffee and Campbell, 1949; Jaffee et al., 1950). The strain of the sintered Ti-6Al-7Nb components is lower with respect to the wrought alloy (10%). This is due to the presence of the residual pores which act as stress concentration sites and to the higher oxygen content of the sintered Ti-6Al-7Nb components in comparison to the wrought Ti-6Al-7Nb alloy. Nonetheless, similar results in terms of strain (1-3 %) were obtained when casting the Ti-6Al-7Nb alloy in a silica-based mould (Kobayashi et al., 1998).

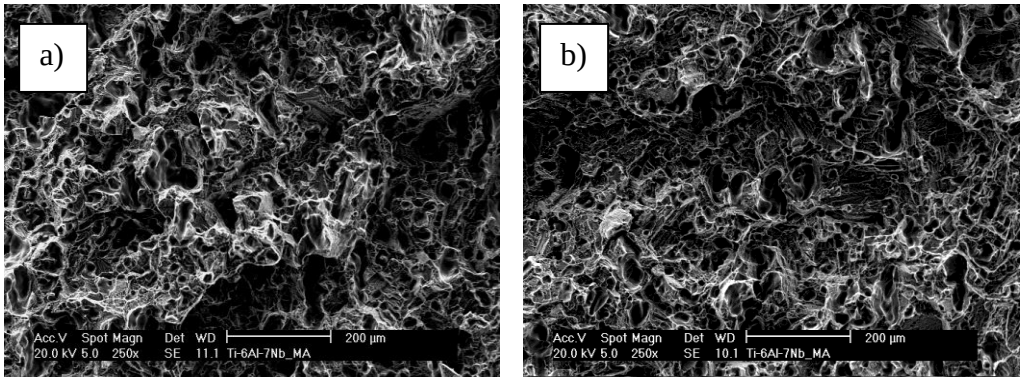

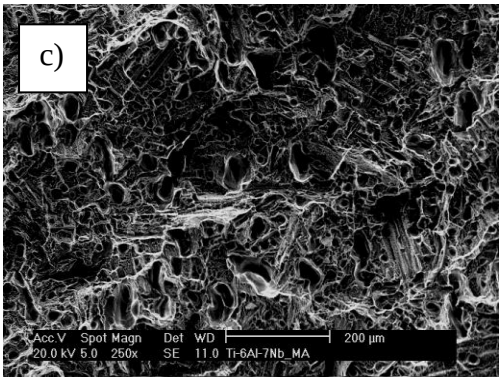

Figure 6. Scanning electron micrographs of the fracture surface of the sintered Ti-6Al-7Nb alloy: a) 1250ºC, b) 1300ºC and c) 1350ºC.

Fractographic results (Figure 6) indicate that the sintered Ti-6Al-7Nb alloy failed in a ductile way via the mechanism of microvoids coalescence as the fracture surfaces are composed by dimples. This is in agreement with the stress-strain curves shown in Figure 5 a). From the shape of dimples found in the fracture surface, dimples which are either conical or elongated, it is inferred that they were generated from the residual porosity leading to the pore-assisted fracture of the sintered alloys. During the analysis, no cleavage zones could be found in the fracture surfaces. The shape of the dimples becomes more spherical/conical or less elongated and their size slightly bigger with the increment of the sintering temperature as the residual porosity was found to decrease in amount and growth in size. As per the fractographic analysis, the elongation at fracture should continuously increase with the reduction of the residual porosity. Nevertheless, the elongation at fracture is negatively affected by the slight increase in oxygen content as discussed earlier.

The study of the mechanical properties of the sintered Ti-6Al-7Nb alloys via quasi-static tensile tests showed that the strength and the fracture mode are similar to those of the wrought Ti-6Al-7Nb alloy but affected by the presence of the residual porosity. Dynamic properties such as fatigue strength of the sintered Ti-6Al-7Nb alloys, which are important for some

structural biomedical applications, will also be lowered by the presence of the residual porosity.

As indicated in the experimental procedure, the dynamic elastic modulus was considered and measured by means of an ultrasonic transducer. The dynamic elastic modulus measurements carried out on the sintered Ti-6Al-7Nb tensile samples results to be quite similar for the three sintering temperatures. The individual values obtained are in the order of 100 MPa giving a mean value of 101±5 GPa which is very similar to the typical value of 105 GPa of wrought Ti-6Al-7Nb alloy (Boyer et al., 1998). This result indicates that there is not a great influence from the level of relative density obtained and this is because, as shown in Figure 2, with the processing parameters employed in this study, the pore structure is mainly composed by relatively small, spherical and isolated pores.

4. Conclusions

From this study about the production and evaluation of the mechanical properties of powder metallurgy Ti-6Al-7Nb alloy obtained means of the press and sinter route, the following conclusions can be drawn:

- Irregular hydride-dehydride powders can successfully be shaped into pressed components which can be handled without fracture;
- The sintering temperatures studied permitted to obtain fully homogeneous microstructures that is paramount as the presence of undissolved particles would affect the biological response of the material;
- The total shrinkage increases from 7.4% to 10.7% and the porosity levels decreases from 6.2% to 4.7% with the increment of the temperature. The pores left after sintering would be beneficial to promote bone osteointegration;
- The mechanical behaviour of the sintered alloys is mainly comparable to that of the wrought alloy as Vickers hardness values of 280-300 HV30, elastic modulus of 101

GPa, ultimate tensile strength around 900 MPa and ductile fracture are achieved. Nevertheless, the elongation at fracture (3%) is affected by the presence of the residual porosity and the high oxygen content of the sintered materials;

- The powder metallurgy master alloy addition approach can successfully be used to process wrought-equivalent titanium biomaterials and therefore is a promising alternative for the manufacturing of non-critical and structural biomedical applications.

Acknowledgements

The authors want to acknowledge the financial support from New Zealand Ministry of Business, Innovation and Employment (MBIE) through the UOWX1402 research contract (TiTeNZ - Titanium Technologies New Zealand).

References

Abkowitz, S., Rowell, D., 1986. Superior Fatigue Properties for Blended Elemental P/M Ti-6Al-4V. Journal of Metals 38, 36-39.

Bolzoni, L., Ruiz-Navas, E.M., Gordo, E., 2013. Flexural Properties, Thermal Conductivity and Electrical Resistivity of Prealloyed and Master Alloy Addition Powder Metallurgy Ti-6Al-4V. Materials and Design 52, 888-895.

Bolzoni, L., Ruiz-Navas, E.M., Neubauer, E., Gordo, E., 2012. Mechanical Properties and Microstructural Evolution of Vacuum Hot-pressed Titanium and Ti-6Al-7Nb Alloy. Journal of the Mechanical Behavior of Biomedical Materials 9C, 91-99.

Boyer, R., Welsch, G., Collings, E.W., 1998. Materials Properties Handbook: Titanium Alloys, in: International, A. (Ed.), 2nd ed, Ohio, USA.

Finlay, W.L., Snyder, J.A., 1950. Effects of Three Interstitial Solutes (Nitrogen, Oxygen and Carbon) on the Mechanical Properties of High-purity Alpha Titanium. Journal of Metals 188, 277-286.

Fujibayashi, S., Neo, M., kim, H.-M., kokubo, T., Nakamura, T., 2004. Osteoinduction of Porous Bioactive Titanium Metal. Biomaterials 25, 443-450.

German, R.M., 1994. Powder Metallurgy Science, 2nd Edition ed. MPIF - Metal Powder Industries Federation, Princeton, USA.

Henry, D., 2009. Materials and Coatings for Medical Devices: Cardiovascular. ASM International, Ohio, USA.

Hulbert, S.F., Morrison, S.J., Klawitter, J.J., 1972. Tissue Reaction to Three Ceramics of Porous and Non-porous Structures. Journal of Biomedical Materials Research 6, 347-374.

Hurless, B.E., Froes, F.H., 2002. Lowering the Cost of Titanium. The AMPTIAC Quarterly 6, 3-10, available at: http://infohouse.p12ric.org/ref/32/31611.pdf (last access November 32016).

Itoh, Y., Miura, H., Sato, K., Niinomi, M., 2007. Fabrication of Ti-6Al-7Nb Alloys by Metal Injection Molding. Materials Science Forum Progress in Powder Metallurgy, Pts 1 and 2, 357-360.

Ivasishin, O.M., 2005. Cost-effective Manufacturing of Titanium Parts with Powder Metallurgy Approach. Materials Forum 29, 1-8.

Jaffee, R.I., Campbell, I.E., 1949. The Effect of Oxygen, Nitrogen and Hydrogen on Iodide Refined Titanium. Transactions of the American Institute of Mining and Metallurgical Engineers 185, 646-654.

Jaffee, R.I., Ogden, H.R., Maykuth, D.J., 1950. Alloys of Titanium with Carbon, Oxygen and Nitrogen. Transactions of the American Institute of Mining and Metallurgical Engineers 188, 1261-1266.

Khan, M.A., Williams, R.L., Williams, D.F., 1996. In-vitro Corrosion and Wear of Titanium Alloys in the Biological Environment. Biomaterials 17, 2117-2126.

Khan, M.A., Williams, R.L., Williams, D.F., 1999. The Corrosion Behaviour of Ti-6Al-4V, Ti-6Al-7Nb and Ti-13Nb-13Zr in Protein Solutions. Biomaterials 20, 631-637.

Kobayashi, E., Wang, T.J., Doi, H., Yoneyama, T., Hamanaka, H., 1998. Mechanical Properties and Corrosion Resistance of Ti-6Al-7Nb Alloy Dental Castings. Journal of Materials Science: Materials in Medicine 9, 567-574.

Long, M., Rack, H.J., 1998. Titanium Alloys in Total Joint Replacement - A Materials Science Perspective. Biomaterials 19, 1621-1639.

Murray, J.L., 1987. Phase Diagrams of Binary Titanium Alloys, 1st ed. ASM International.

Narayan, R., 2009. Biomedical Materials. Springer.

Niinomi, M., 1998. Mechanical Properties of Biomedical Titanium Alloys. Materials Science and Engineering A 243, 231-236.

Niinomi, M., 2002. Recent metallic materials for biomedical applications. Metallurgical and Materials Transactions A 33, 477-486.

Schatt, W., Wieters, K.-P., 1997. Powder Metallurgy. Processing and Materials. EPMA - European Powder Metallurgy Association, Shrewsbury, UK.

Semlitsch, M., Staub, F., H., W., 1985. Titanium-aluminium-niobium Alloy Development for Biocompatible, High Strength Surgical Implants. Biomedizinische Technik/Biomedical Engineering 30, 334–339.

Semlitsch, M., Weber, H., Steger, R., 1995. Fifteen Years Experience with Ti-6AI-7Nb Alloy for Joint Replacements, in: Blenkinsop, P.A., Evans, W. J., Flower, H. M. (Ed.), Titanium '95: Science and Technology, Birmingham - UK, pp. 1742-1759.

Semlitsch, M.F., Weber, H., Streicher, R.M., Schön, R., 1992. Joint Replacement Components Made of Hot-forged and Surface-treated Ti-6Al-7Nb Alloy. Biomaterials 13, 781-788.